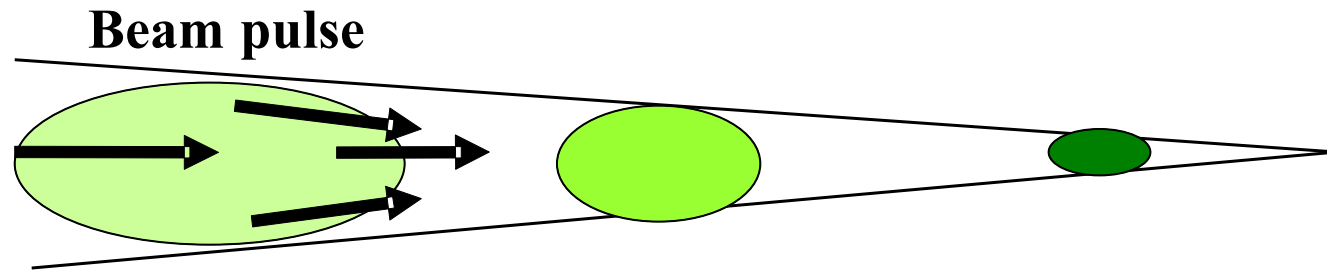


Drift Compression and Final Focus

- Igor D. Kaganovich, James Mitrani, Edward A. Startsev, and Ronald C. Davidson,
– *Princeton Plasma Physics Laboratory*
- Mikhail A. Dorf and Alex Friedman
– *Lawrence Livermore National Laboratory*
- Steven M. Lidia, Jean-Luc Vay, and Peter Seidl
– *Lawrence Berkeley National Laboratory*
- Scott Massidda, Columbia University
- William Berdanier, University Texas at Austin

Neutralized drift compression can potentially reach $300 \times 900 \sim 3 \times 10^5$ combined longitudinal and transverse compression of ion beam pulse



If all ions of the beam pulse are ideally focused to one spot the final compression is limited by small temperature or emittance.

An example:

1 meter length pulse longitudinally to 3 mm=>

300 density compression

3 cm radius beam compression to 1 mm =>

$30^2=900$ density compression.

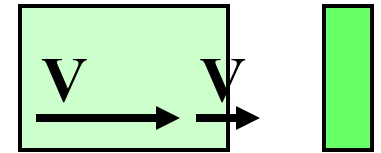
#3

Outline: Drift Compression and Final Focus

- Longitudinal drift compression
 - Effects of voltage errors
- Simultaneous longitudinal and radial compression
 - Chromatic effects in final focus
- Physics of the neutralization process and requirements for plasma sources.

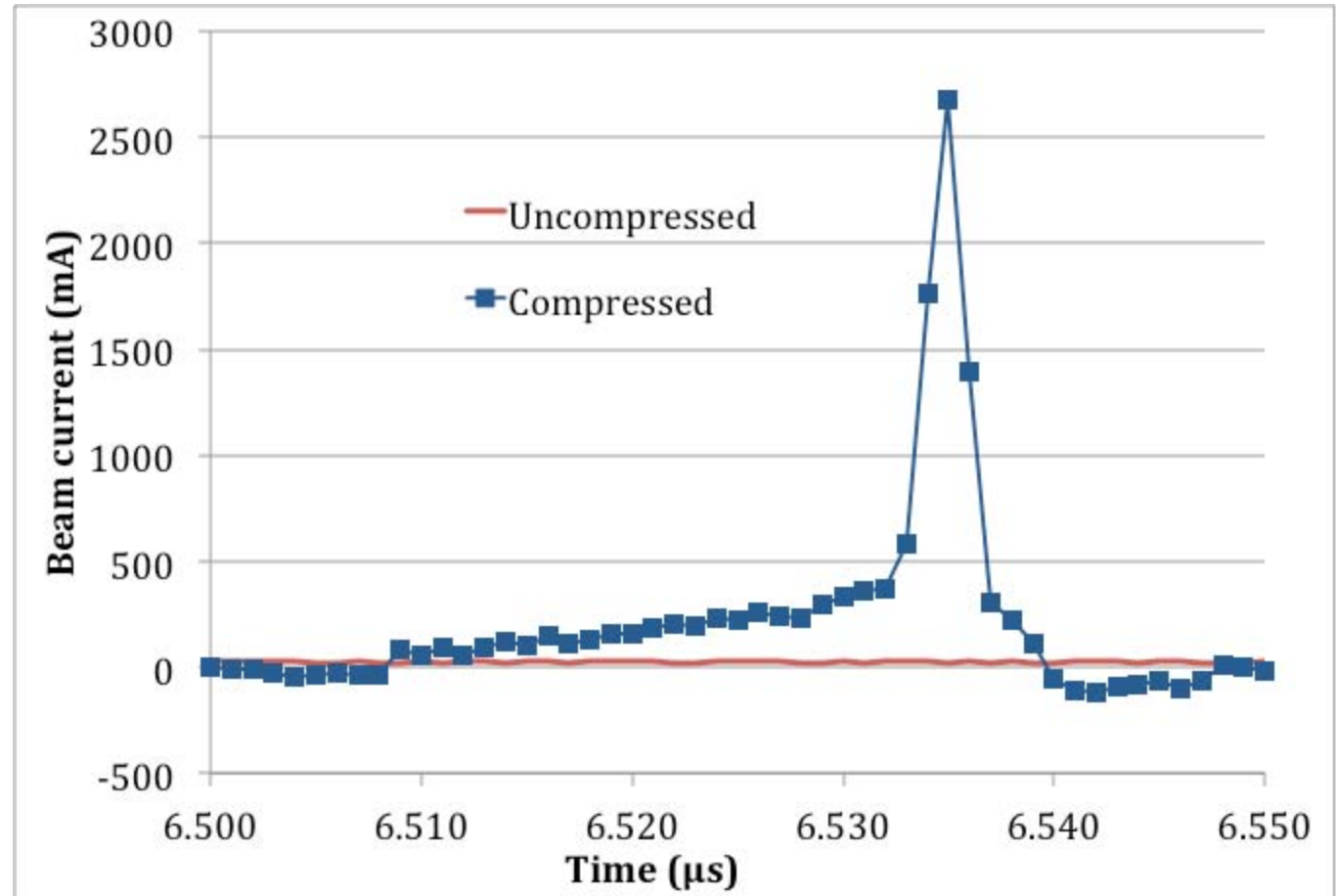
#4

Longitudinal Compression

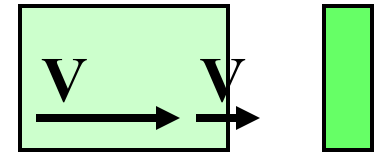


Experiments on NDCX-I observed ~ 90 times compression: the peak current (2.7A) increased from the uncompressed current (0.030A).

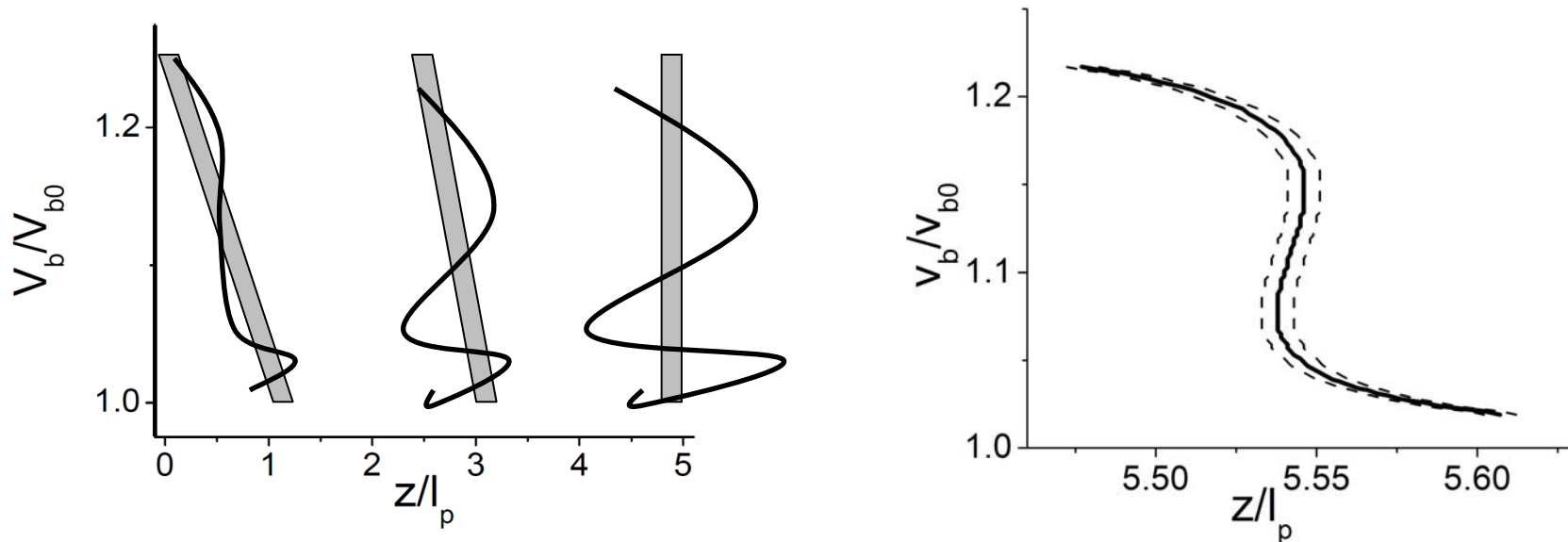
S. Lidia et al,
PAC Proceedings
(2011).



#5 Longitudinal Compression is sensitive to errors in velocity tilt



The phase-space during ideal compression with a linear velocity gradient.



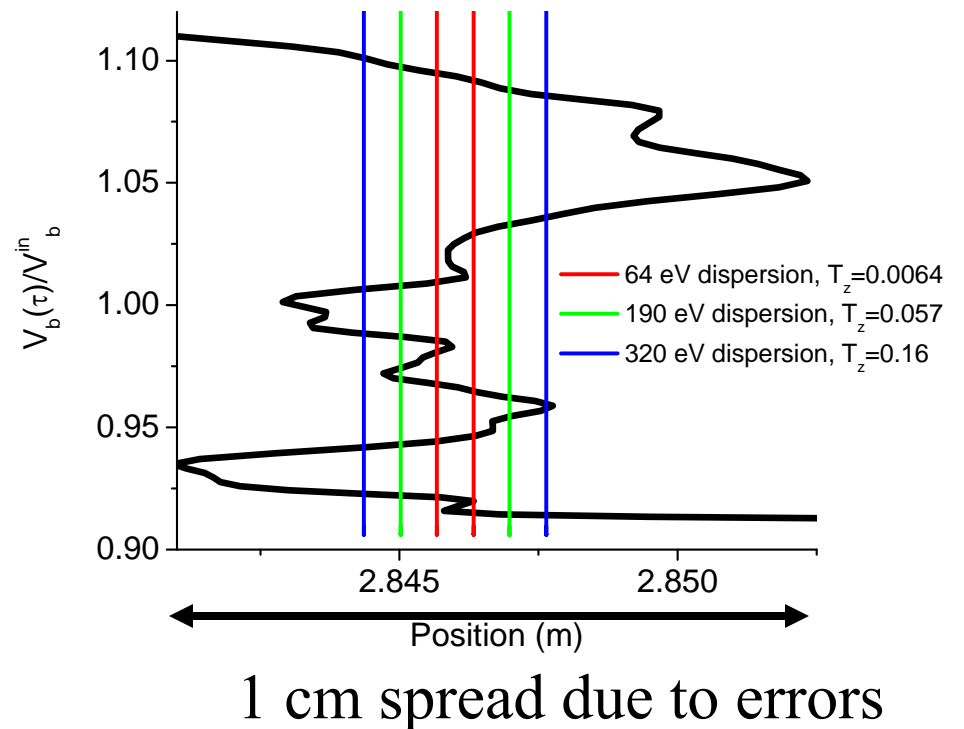
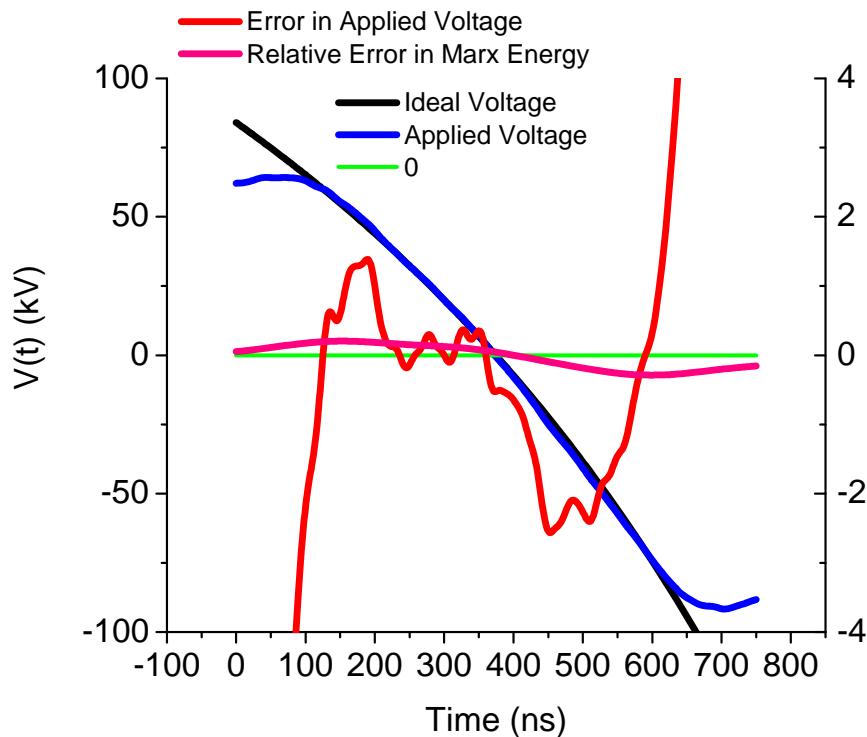
Compression time given by $1/(dv/dz)$ is very sensitive to small scale wiggles, that result in different parts of the beam pulse being compressed at different locations.

#6

1-10% Voltage errors limit the longitudinal compression

Experimental voltage waveform of the NDCX-I induction bunching module from S. Massida et al., NIMA **678**, 39 (2012).

Phase space plot of the pulse with different mean intrinsic energy spreads; $E_{b0} = 322\text{keV}$, and the target location is at $z=2.846\text{m}$.

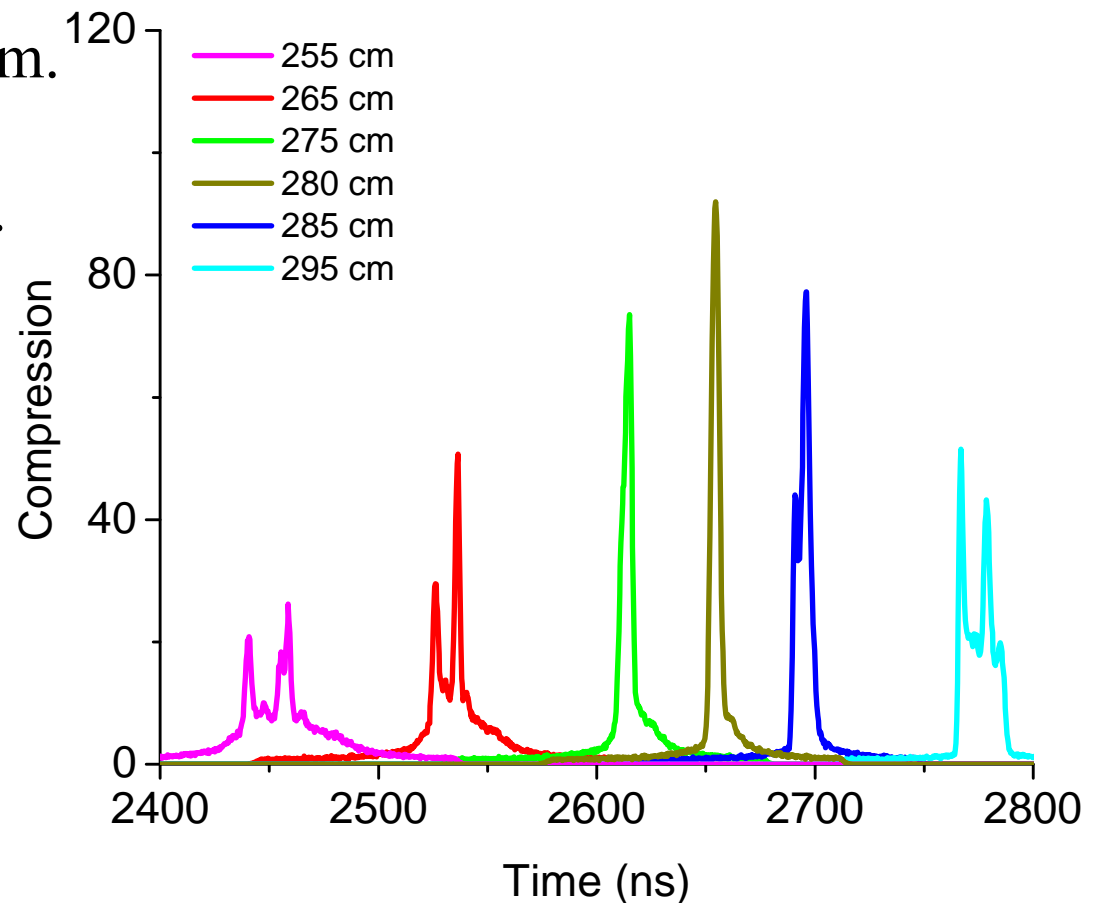


#7 Beam compresses for a wide range of locations near the target plane

The simulated compressed pulse waveform at six different target locations, from $z=255$ cm to 295 cm as a function of drift time for the NDCX-I voltage waveform.

The beam energy is 317keV,
the energy spread is 252eV*.

* From S. Massidda, et al,
NIMA **678**, 39 (2012).



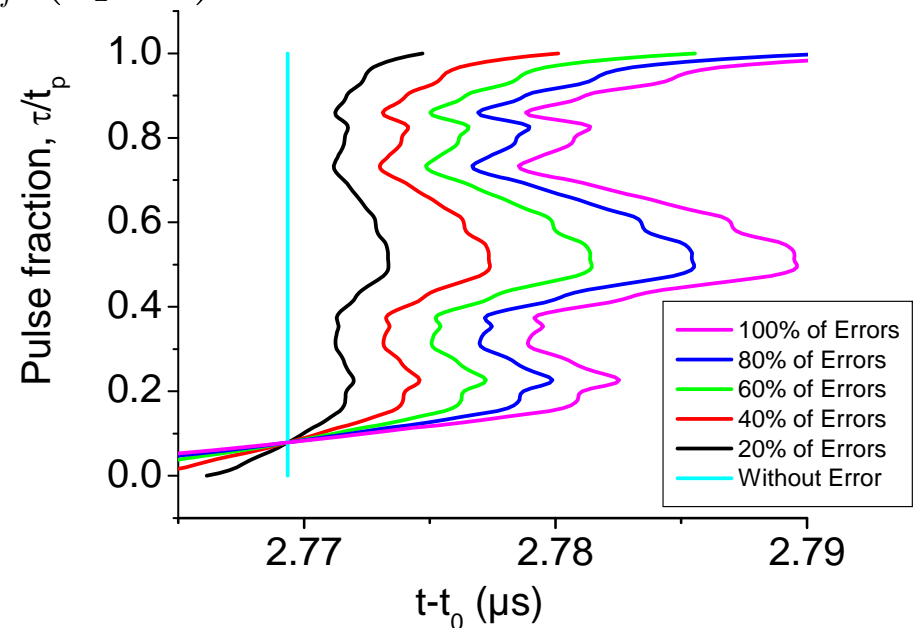
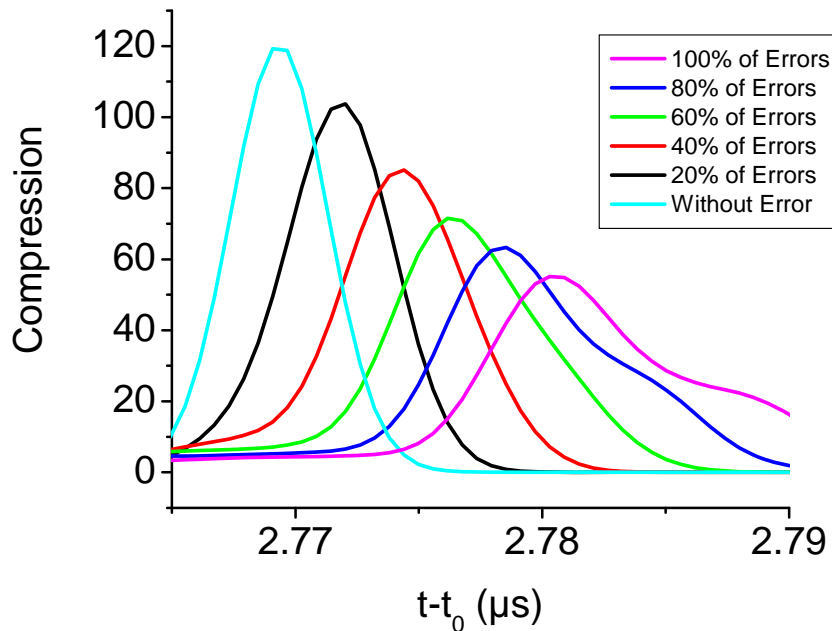
#8

Compression ratio is a weak function of errors; a factor of two improvement will require a lot of work

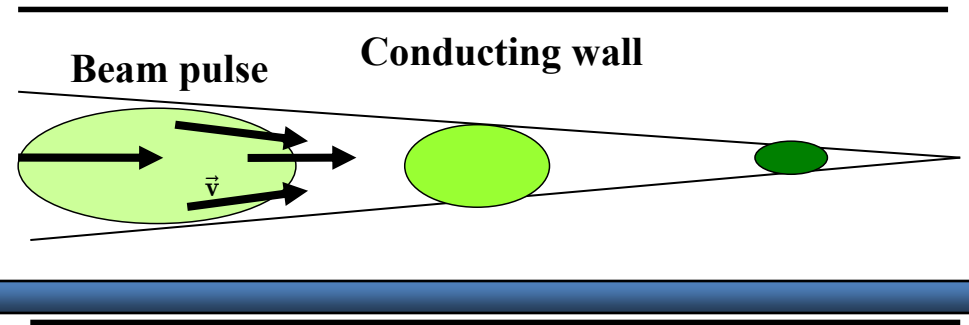
Simulated compressed pulse waveform and pulse location at the target location for reduced voltage errors as a function of time.

The initial beam energy is 276keV, and the longitudinal temperature is $T_z=0.27\text{eV}$

$$C_{\text{max}} \approx \frac{\tau_\gamma}{t_f} \left(\frac{v_b E_b}{v_T \delta U} \right)^{1/2}$$



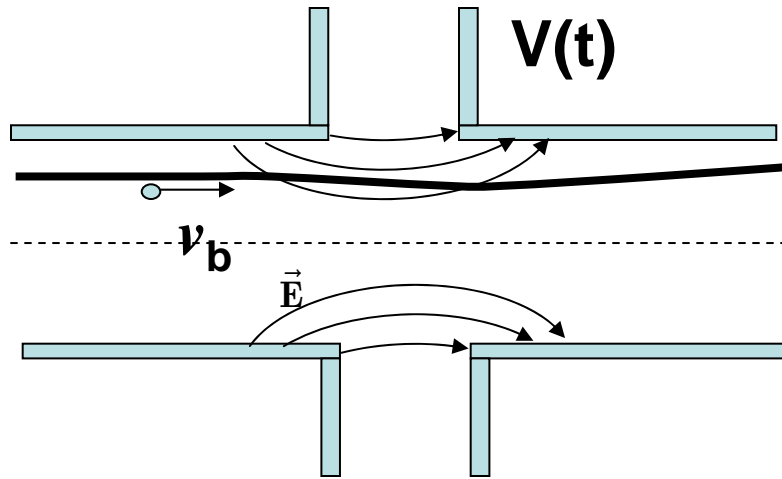
Outline



- Longitudinal Drift compression
 - Effects of voltage errors
- Simultaneous longitudinal and radial compression
 - Chromatic effects in final focus region

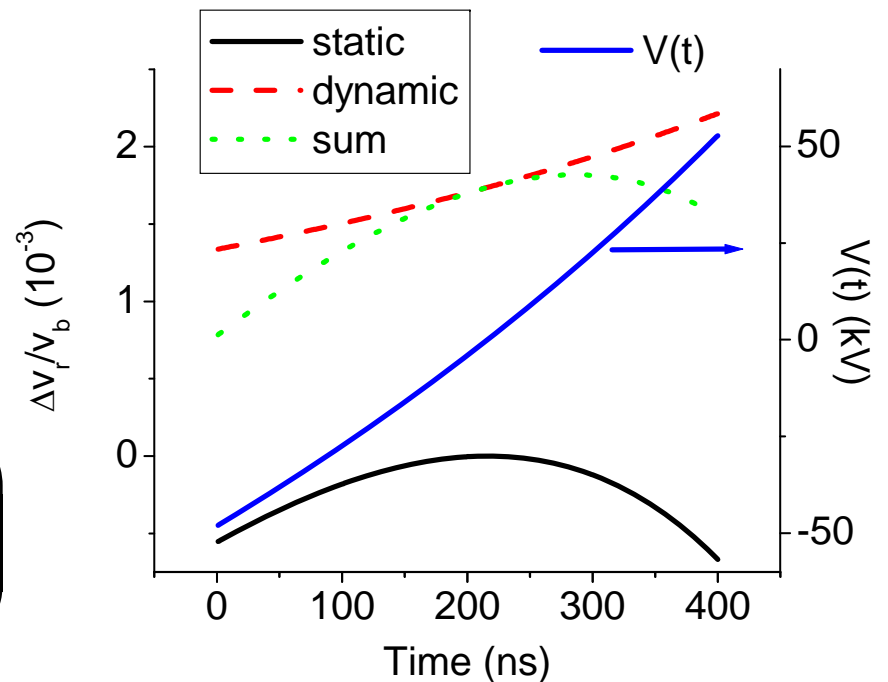
#10 Aberrations in the bunching module results in beam defocusing

Acceleration gap of the induction bunching module.



The static and dynamic aberrations for NDCX-I. Pulse length $t_p=400\text{ns}$, $E_b=300\text{keV}$, $r=1\text{cm}$, $R_w=3.8\text{cm}$.

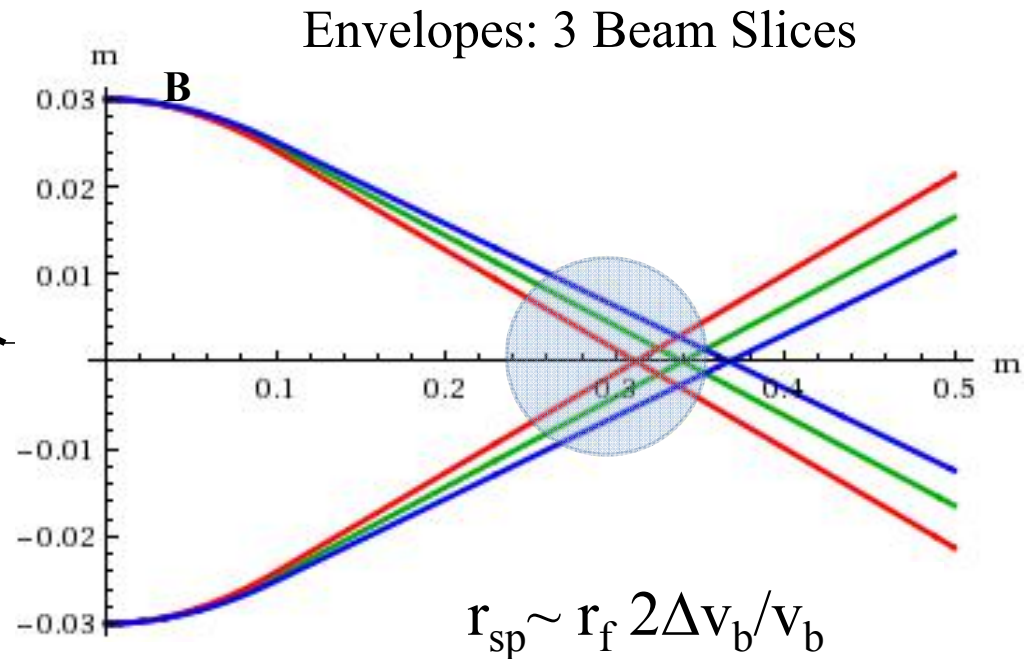
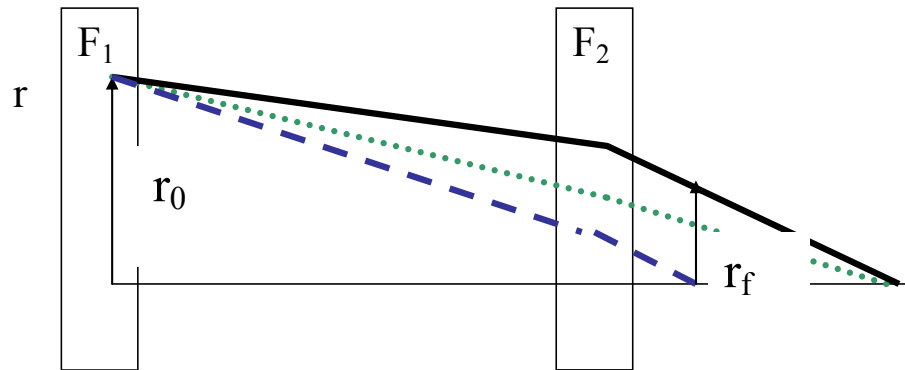
$$\frac{\Delta v_{br}}{v_{b0}} \approx \frac{r}{R_w} \left(-\frac{R_w}{4v_{b0}} \frac{e\dot{V}(t)}{E_b} - 0.082 \left(\frac{eV(t)}{E_b} \right)^2 \right)$$



#11

Strong final focusing element is utilized to reduce spot size at target.

A strong focusing element mitigates defocusing errors in the bunching module, because the beam particles from different radial locations are focused onto the target, but introduces chromatic effects.



#12

Chromatic effects in the final solenoid yield a sharply peaked radial distribution with “long wings”

NCDX-II beam parameters: 8T solenoid, 10% velocity tilt; initial beam radius $R_0=30$ mm; 3 MeV Li^+ ions; $\epsilon=2.25$ mm·mrad.

r_{50} – radius containing 50% of beam particles.

r_{90} – radius containing 90%.

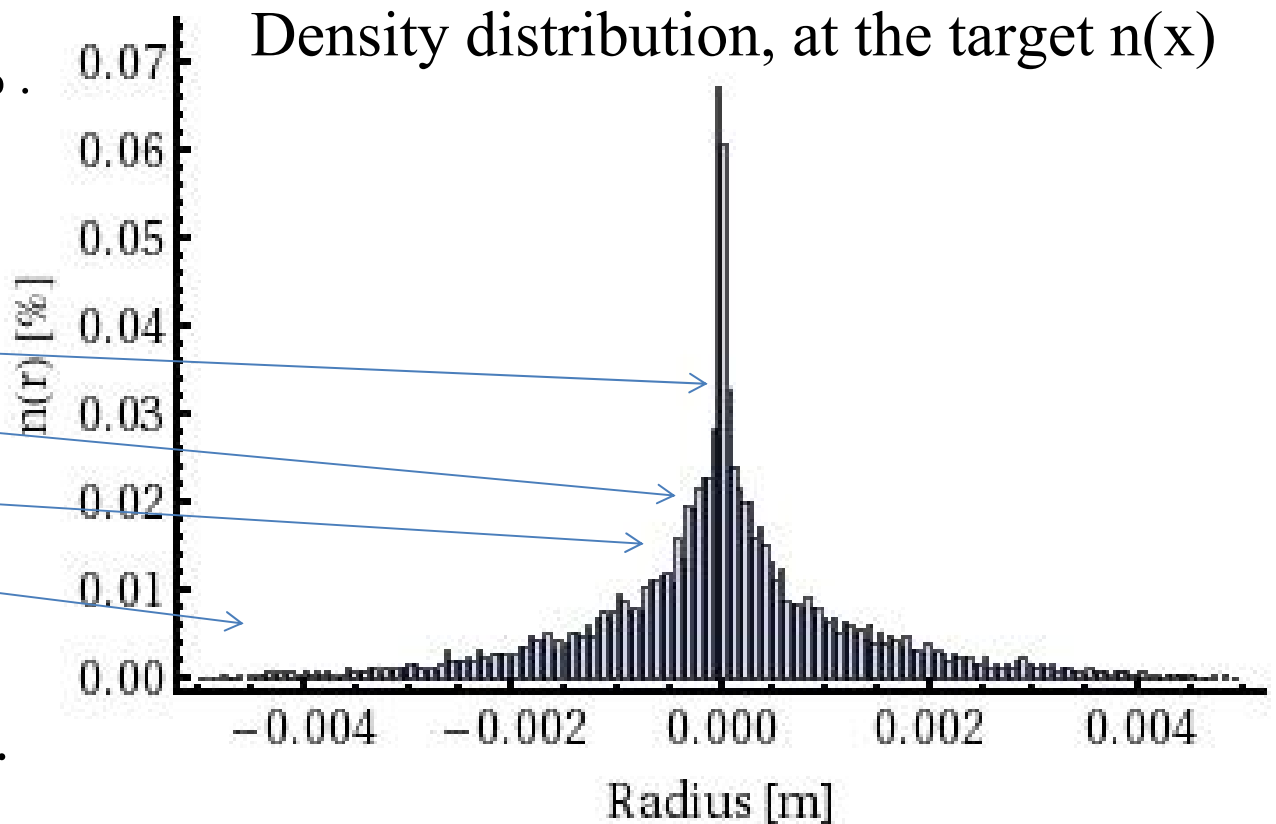
r_{100} – radius containing 100% .

FWHM $\approx 150\mu\text{m}$.

$r_{50} = 540\mu\text{m}$.

$r_{90} = 1.57$ mm.

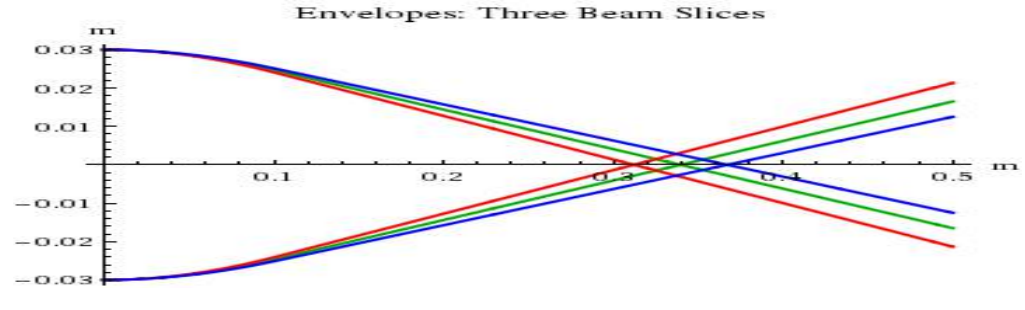
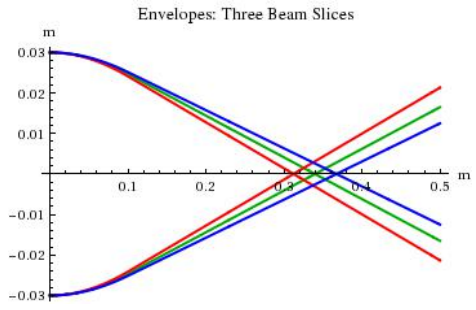
$r_{100} = 5.66$ mm.



J. Mitrani, et al (2012).

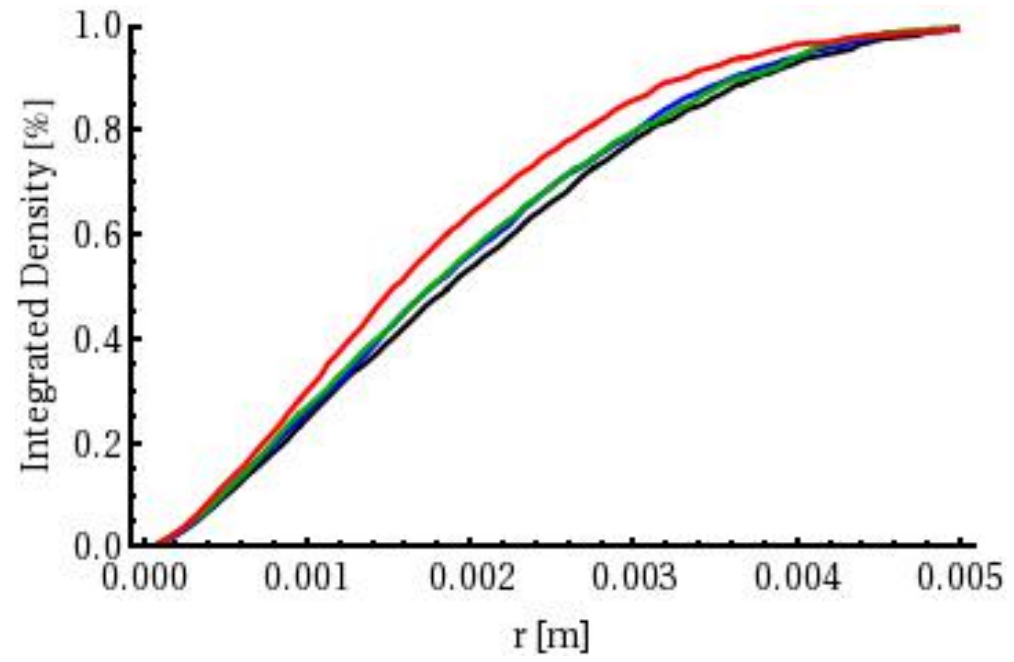
#13

Increasing strength of final solenoid does not reduce the spot size $r_{sp} \sim r_f 2\Delta v_b/v_b$



Density distribution, $n(x)$ at the target

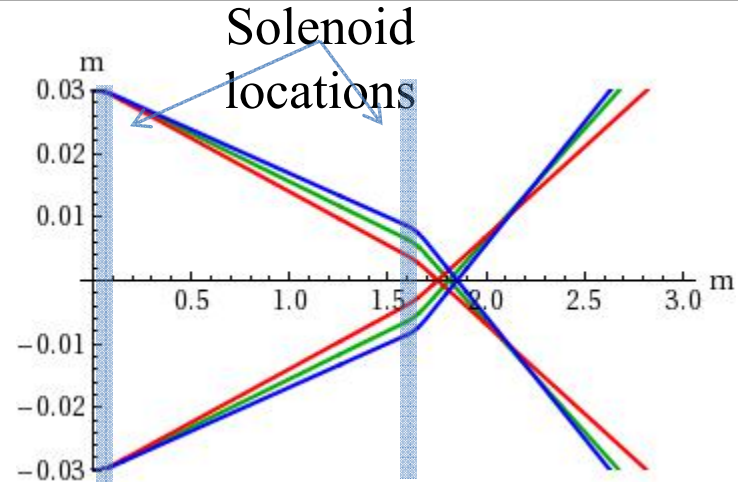
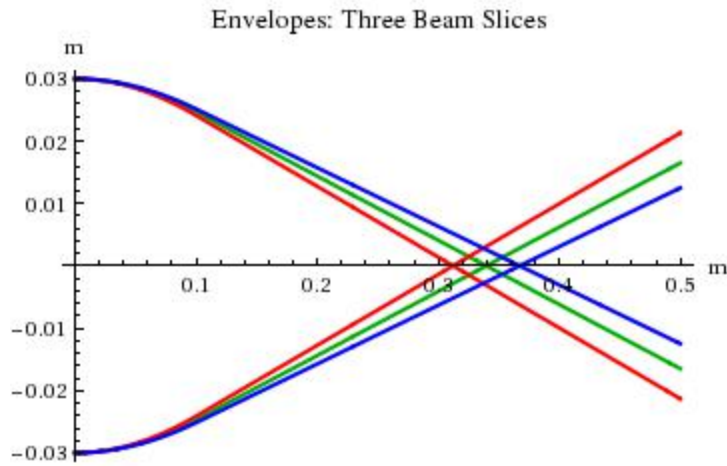
Black/blue/green/red curves represent FFS field strengths of 3, 8, 12, & 16T, respectively.



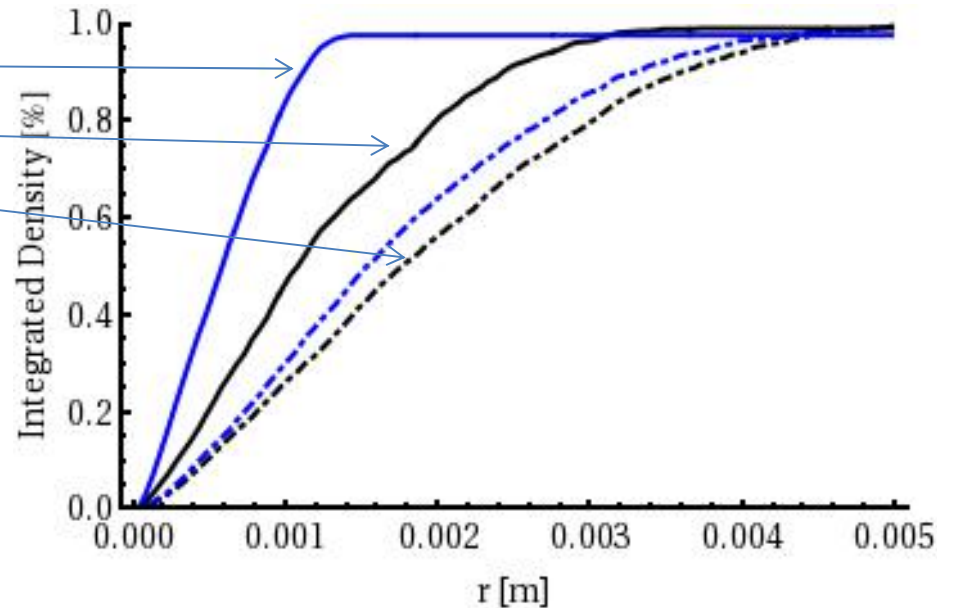
J. Mitrani, et al (2012).

#14

Using two solenoids yields about a twice smaller spot size=100s micron! $r_{sp} \sim r_f 2\Delta v_b/v_b$



	One 8T FFS	One 16T FFS	2 Sol – 3 & 8T	2 Sol – 3 & 16T
FWHM μm	150	250	250	150
Fwhm [%]*	15.2	23.1	31.6	15.6
R_{50} [μm]	540	479	289	166
R_{90} [mm]	1.57	1.37	0.86	0.49
R_{100} [mm]	5.66	4.95	3.08	1.08



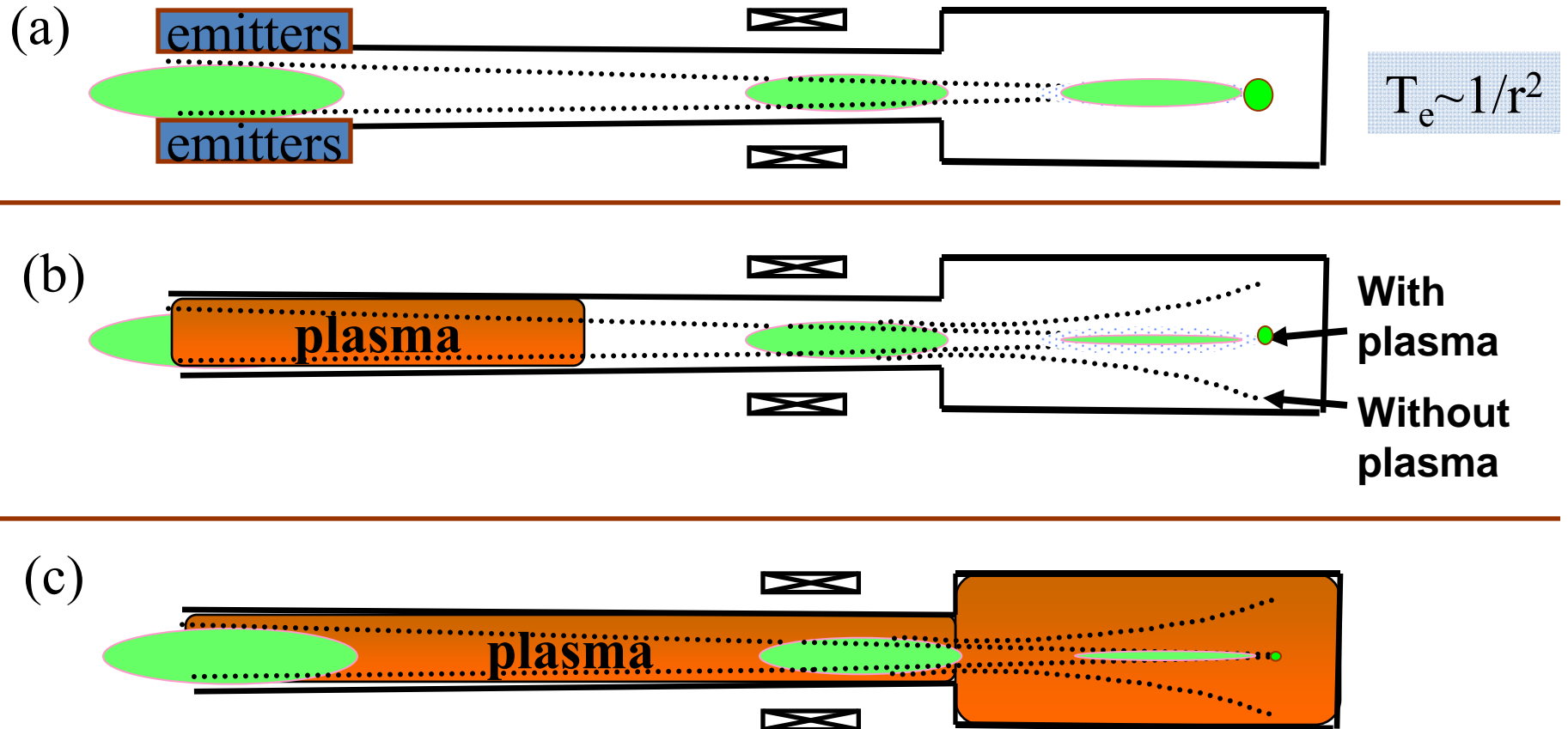
Outline

- Longitudinal Drift compression
 - Effects of voltage errors
- Simultaneous longitudinal and radial compression
 - Chromatic effects in final focus
- **Physics of the neutralization process and requirements for plasma sources.**

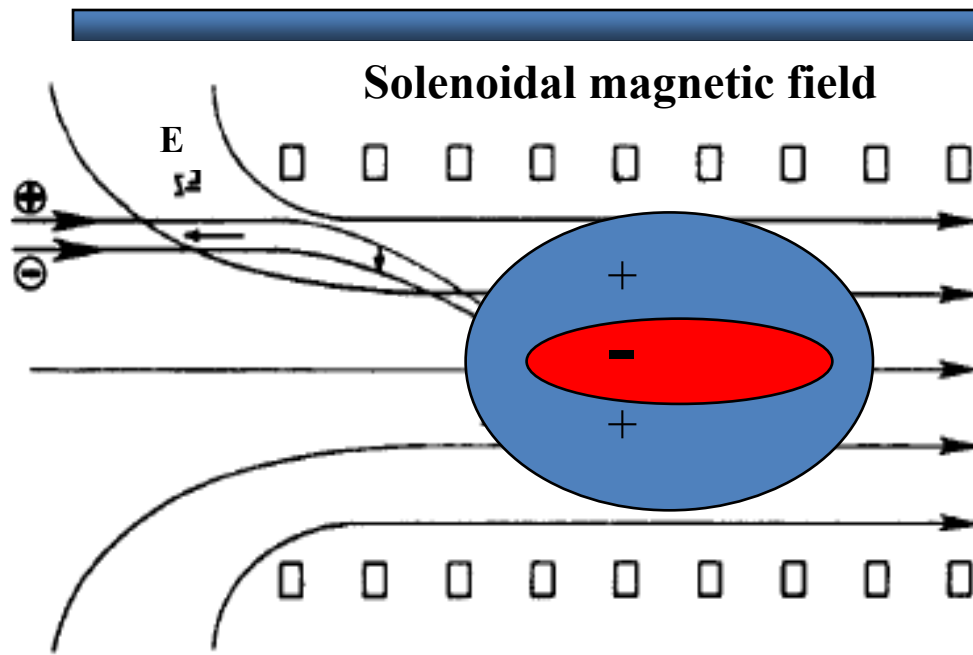
Methods to neutralize intense ion beams

I. D. Kaganovich et al., Physics of neutralization of intense high-energy ion beam pulses by electrons, Phys. Plasmas **17**, 056703 (2010).

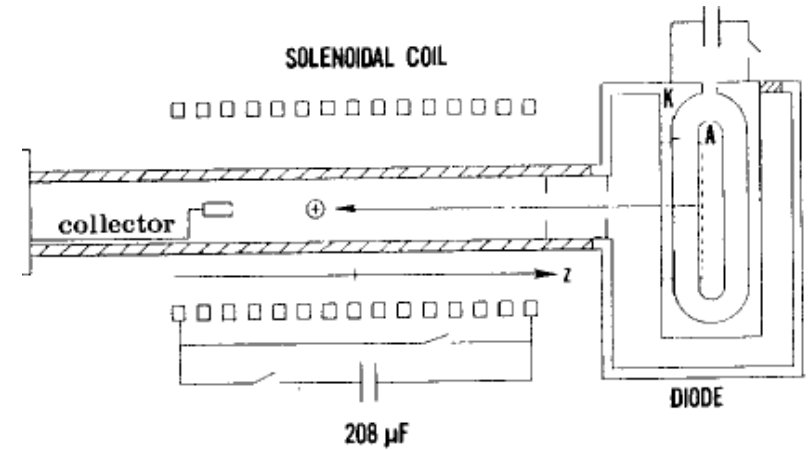
(a) emitters, (b) plasma plug, and (c) plasma everywhere



Collective focusing schemes



$E_b \sim 360 \text{ keV}, r_b \sim 2 \text{ cm}, n_b \sim 1.5 \cdot 10^{11} \text{ cm}^{-3}$



. Experimental apparatus.

S. Robertson, PRL **48**, 149 (1982). Thin collective lens

From R. Kraft, Phys. Fluids **30**, 245 (1987).

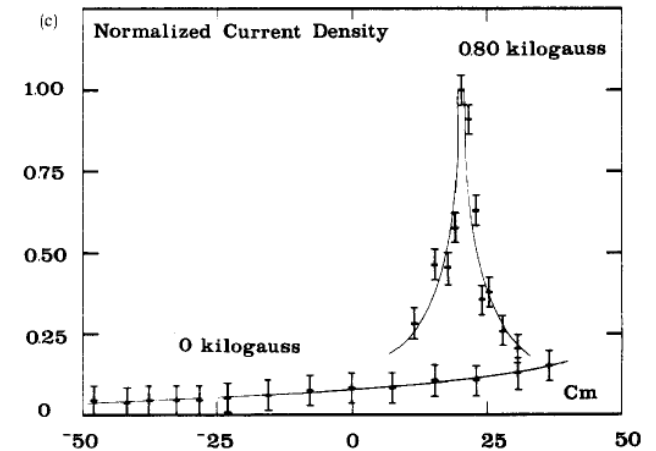
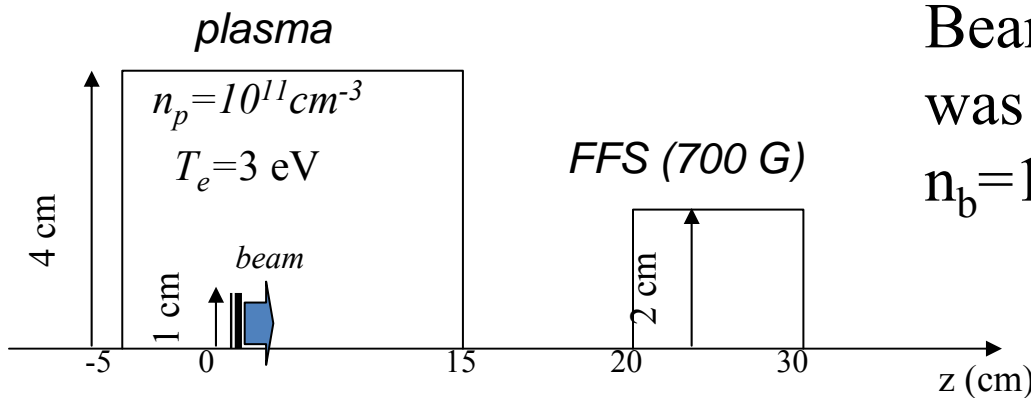


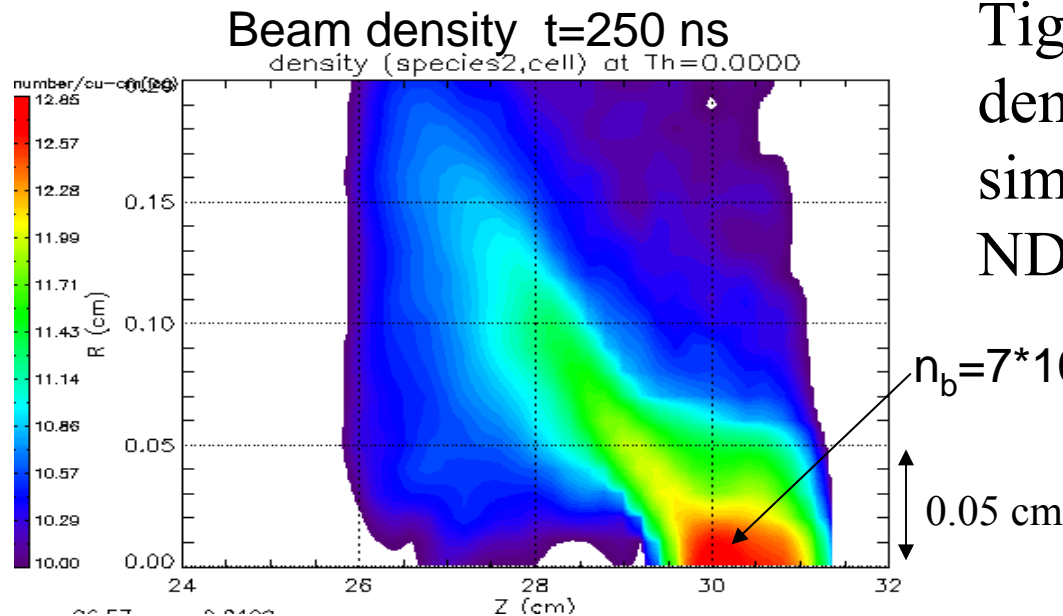
FIG. 8. Focused ion current. (a) Ion current density versus time ($B = 0, 1.5 \text{ kG}$). (b) Peak ion current density versus axial position ($B = 0, 1.5 \text{ kG}$). (c) Peak ion current density versus axial position ($B = 0, 1.5 \text{ kG}$).

#19

PIC Simulations Show Collective Focusing Lens can be Used for NDCX Beam Final Focus*



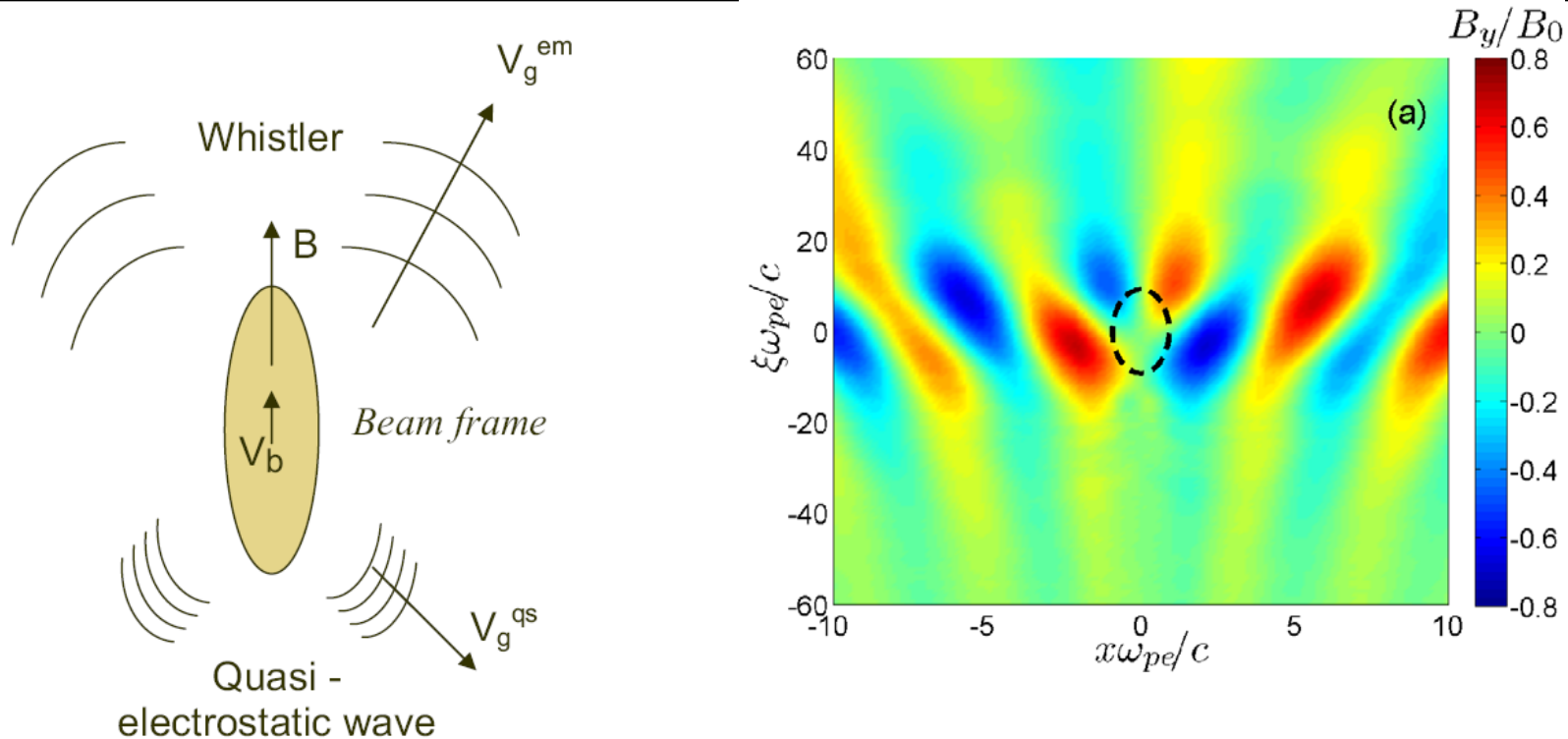
Beam pulse K^+ 320keV, $r_b=1$ cm, was compressed 700 times from $n_b=10^{10} \text{cm}^{-3}$ to $n_b=7 \cdot 10^{12} \text{cm}^{-3}$!



Tight final focus $r_f < 1$ mm was demonstrated in PIC (LSP) simulations for both NDCX-I and NDCX-II.

*M. Dorf, I. Kaganovich, E. Startsev, and R. Davidson, PoP 19, 056704 (2012).

The beam can excite whistler waves



Whistler waves can be excited by the ion beam pulse.

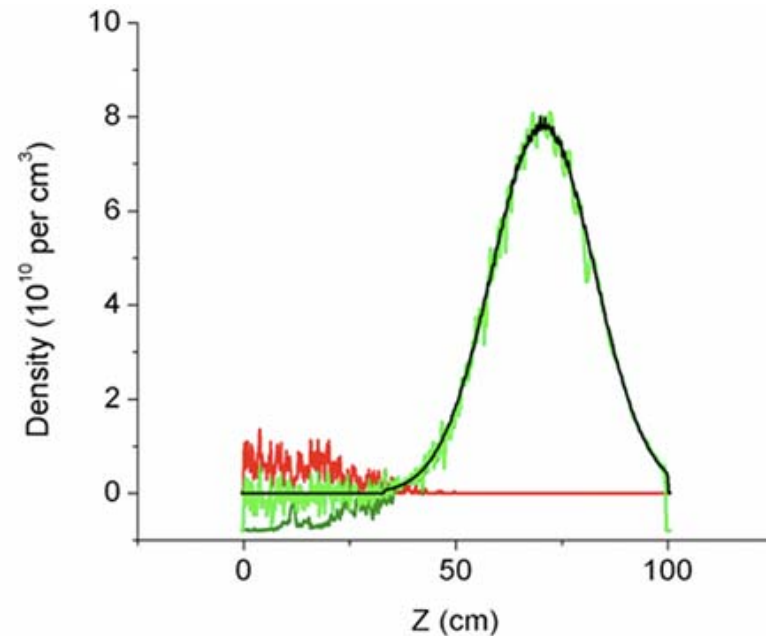
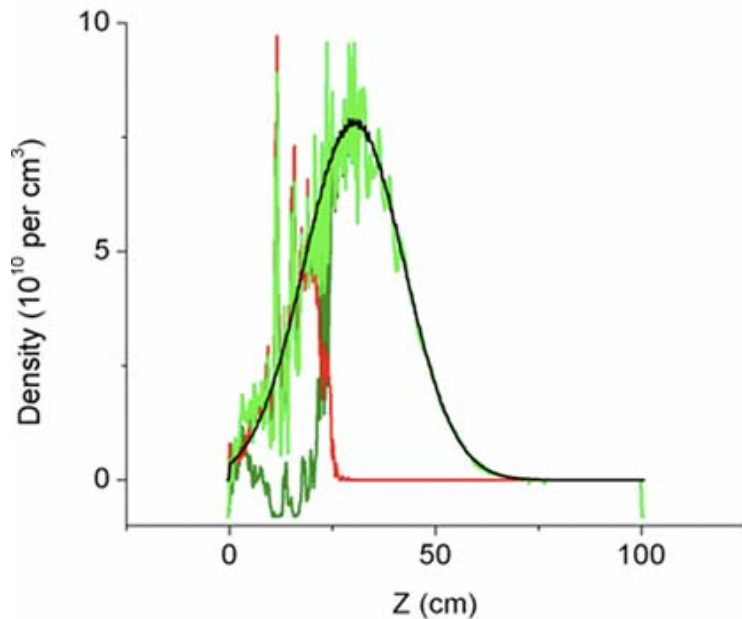
M. Dorf et al., Phys. Plasmas **17**, 023103 (2010).

Strong (resonant) wave excitation occurs at $\omega_{ce}/2\beta_b\omega_{pe}=1$.

Tenuous plasma from large volume can provide sufficient neutralization and avoid two-stream instability.



Density slices along $r = 2$ cm; black is beam ion density; red is emitted electron density; dark green is plasma electron density; and bright green is the sum of the red and dark green curves.



William Berdanier et al. (2011)

Conclusions for Neutralized Drift Compression and Final Focus

Longitudinal compression is limited by errors in the applied velocity tilt and is not affected by plasma neutralization.

The radial compression is mostly limited by chromatic effects in the focusing system. Two-solenoid scheme provide better focusing than one-solenoid scheme. Inadequate neutralization and instabilities may affect focusing as well.

The applied magnetic field tends to increase the self-consistent radial electric field and can be actively used for beam focusing in various collective focusing schemes. However, collective focusing can also be subject to instabilities and deleterious effects.